THROUGH THE WALL

High-precision machines often require a high vacuum level. Contamination due to moving cables and bearings of the positioning stages within is an issue, which can be solved using an inverted planar motor [1]. However, this solution leads to a complex system due to position-dependent commutation and a large number of coils. An alternative stage design was made at MI-Partners, having a low degree of complexity and minimising contamination of the vacuum: the so-called through-wall stage.

DICK LARO, ELWIN BOOTS, JAN VAN EIJK AND LEO SANDERS

In the concept, a separation has been made between two vacuum levels: a clean/precision vacuum and a non-precision/dirty vacuum. The separation between the two is realised by a wall (see Figure 1). The design uses a Short Stroke-Long Stroke (SS-LS) stage configuration where the SS stage exerts its actuation forces through the wall. The precision vacuum contains the SS chuck carrying a wafer to be machined or inspected. In the non-precision vacuum a conventionally stacked LS x-y stage can be placed. The function of this XY stage is to enable a larger stroke for the short-stroke system. The vacuum underneath the separator plate is only required to minimise loads on the wall due to the pressure difference over a large area.

One of the challenges of the “through wall” concept lies in the development of new actuators. These actuators will have to act through the wall. This wall introduces a relatively large airgap. The typical airgap is assumed to be in the order of 5 mm. This 5 mm consists of space for the wall itself and its deflection and allows for a mechanical tolerance of 1 mm on each side.

AUTHORS’ NOTE

Dick Laro, system architect, Elwin Boots, mechatronical developer, and Leo Sanders, director, all work at Eindhoven-based MI-Partners. MI-Partners is a company that performs contract R&D in the field of high-tech mechatronics. This article in part draws on the M.Sc. work by Elwin Boots when he was a Mechanical Engineering student at Delft University of Technology, the Netherlands. Jan van Eijk is professor emeritus of Advanced Mechatronics at Delft University of Technology and is owner of MICE bv, based in Eindhoven, the Netherlands.
This article was, in part, based on a presentation at the DSPE Conference, which was held on 4 and 5 September 2012 in Deurne, the Netherlands.
The authors thank IBS Precision Engineering for supplying the eddy-current sensors and Magnetic Innovations for verifying the 2D simulations in 3D.
This research has been conducted within the XTreme Motion project, part of the “Pieken in de Delta” programme of the Dutch Ministry of Economic Affairs.

d.laro@mi-partners.nl, www.mi-partners.nl, www.micebv.nl, www.tudelft.nl

System architecture

The performance of the through-wall concept has been evaluated by realising a demonstrator. The demonstrator’s machine architecture was based on a separate force frame and sensor frame layout. The schematic layout of the dynamic architecture is shown in Figure 2. The reaction forces of the SS stage are transferred through the LS stage into the force frame. These SS reaction forces could excite internal dynamics within the LS stage, possibly limiting the bandwidth of the SS stage. By placing the sensors on a separate metrology frame with a low-frequency suspension, a mechanical filter is formed that reduces the “visibility” of flexible modes within the force frame and LS stage.

The SS chuck holds the wafer on which machining or inspection can occur. The SS stage is controlled in the six degrees of freedom (DoFs) of a rigid body. For an unconstrained rigid body, a minimum of six sensors and six actuators are needed to control the six DoFs. When more sensors or actuators are used than the number of controlled DoFs, the system is called over-sensed or over-actuated, respectively. A wafer chuck is typically square-shaped. The torsional mode of such a structure typically limits the achievable bandwidth in vertical directions (Z, Rx, Ry). Research [2] has shown that by using four actuators in vertical direction instead of the minimum number of three, the internal dynamics of the chuck are more favourably excited. This allows high bandwidths to be achieved for lighter, more flexible systems. To exploit this advantage, four vertical actuators are used. As a symmetrical mass distribution is beneficial for the applied over-actuation, four horizontal actuators are used as well.

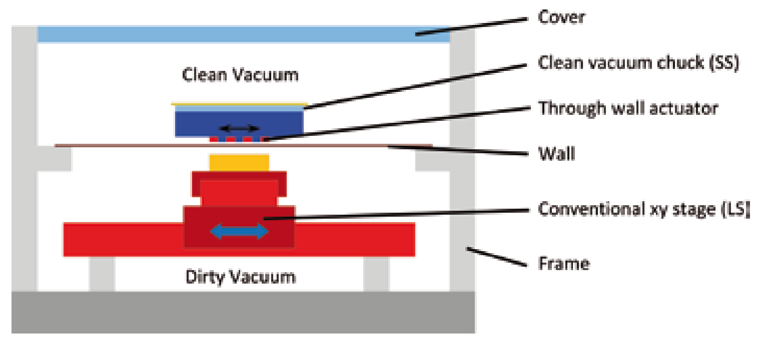

1

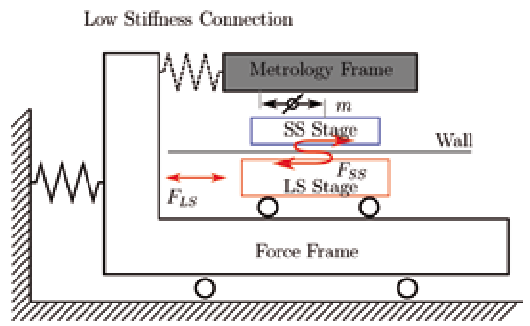

2

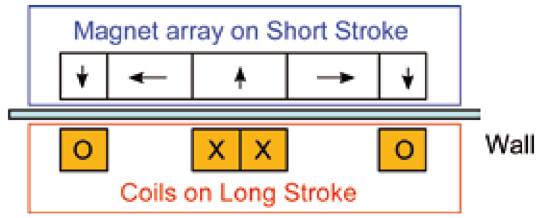

3

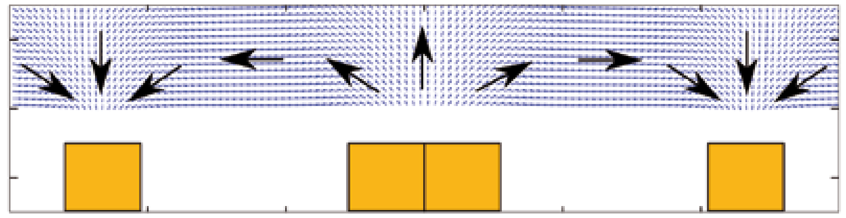

4

The SS is positioned with respect to the metrology frame using active control loops. To minimise transfer of disturbances to the SS stage, the connection in the form of stiffness to the outside world should be kept small. As the stage operates without cables, the dominant stiffness is present within the actuators. One of the goals for the actuator design is to keep the combined stiffness below 3 N/mm.

Actuator design

For the through-wall concept, the airgap will typically be larger than in a conventional system. Next to this, only one side is available for attaching coils. This requires the development of new actuators. To keep control of the stage simple, the goal is to develop 1-DoF actuators that do not require position-dependent control. The design of the actuators is based on “off-the-shelf” magnets to allow for a relatively short manufacturing time.

In-plane design

The in-plane actuator consists of a planar Halbach magnet arrangement and two coils (Figure 3). The Halbach arrangement is attached to the SS stage and “pushes” the magnetic field through the (non-ferromagnetic) wall towards the LS stage. Inside the LS stage the coils are situated. The SS and LS stages make relative displacements in the order of one millimeter. The magnetic design minimises position dependency of the propulsion force.

To optimise the actuator design, analytical equations for square magnets [3] were used. The magnetisation direction for the magnets has to be established within a fixed volume to achieve maximum propulsion force. To do so, the magnet area was divided into 1 mm² blocks, with each block having its own magnetisation direction. For each block the magnetic field is calculated with horizontal and vertical magnetisation using the analytic formulas. The forces in the coil are then calculated by taking the cross product between the current density and the magnetic field. Finally, the total force and torque are calculated by numerical integration over the coil. These forces correspond to the horizontally and vertically magnetised block; other magnetisation directions can be calculated using combinations of the horizontally and vertically magnetised block. The magnet configuration that delivers the highest force is shown in Figure 4.

To be able to use off-the-shelf magnets, the configuration had to be simplified. The final configuration was chosen such that it can be fabricated out of just one type of cuboid magnets. The resulting magnetic field is shown in Figure 5. The design without active coil cooling is capable of generating a propulsion force of 60 N at a gap of 5 mm. When water cooling is applied to the actuator on the LS side and the magnet geometry is customised, the force can easily

1 Through-wall vacuum stage concept, showing the separation between a precision/clean and a non-precision/dirty vacuum compartment, as well as the Long Stroke-Short Stroke stage configuration.

2 Dynamic architecture of the through-wall stage. The reaction forces of the SS pass through the LS stage into the force frame. The metrology frame is isolated with respect to the force frame.

3 In-plane motor concept, with a Halbach array on the SS stage and coils on the LS stage.

4 Optimal magnetic field for coils, to optimise propulsion force.

5 Magnetic field of designed in-plane actuator.

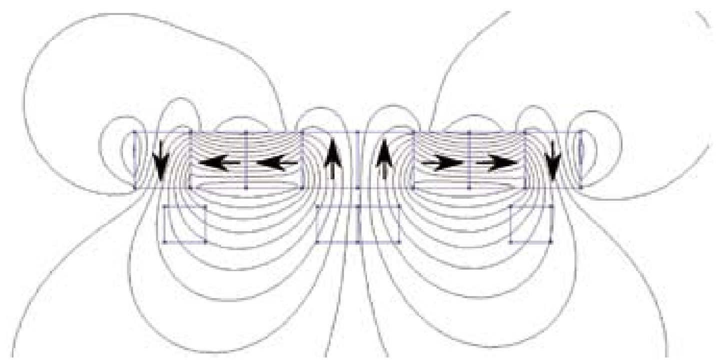

5

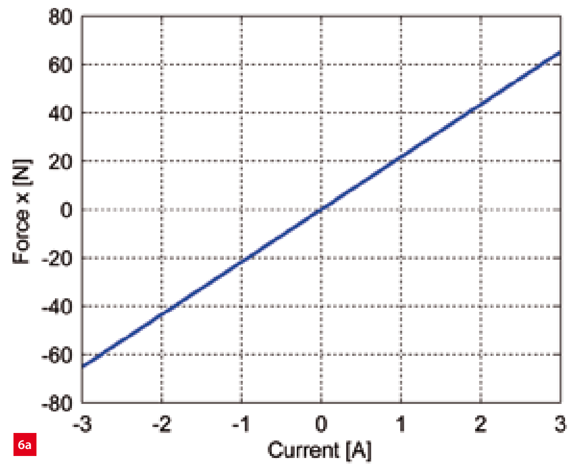

6a

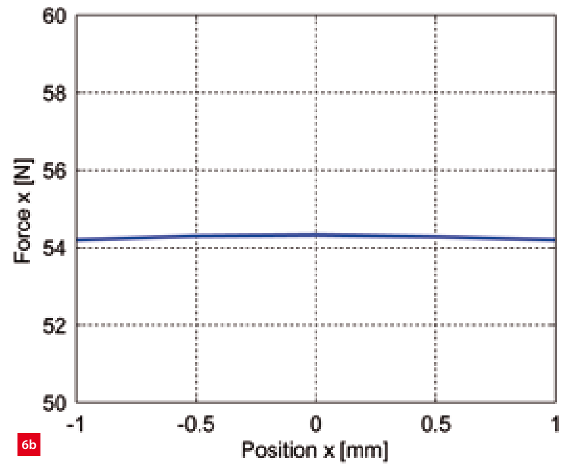

6b

6 *Measured forces of in-plane motor. (a) Force versus current. (b) Force versus position at* ***I*** *= 2.5 A.*
7 *Active magnetic gravity compensator for through-wall concept. Coils are present on LS side.*
8 *Working principle of active magnetic gravity compensator. Zero stiffness realised by ring-shaped magnet.*

be increased by a factor of 4 within the same volume (100 mm x 150 mm x 40 mm). Specialised tools have been developed for actuator assembly, e.g. care should be taken to avoid demagnetisation during assembly.

A measurement set-up has been realised to characterise the actuator. Figure 6 shows the measured force-versus-current characteristics. The position dependency is negligible and less than 1% of the actuation force.

Active magnetic gravity compensator

The active magnetic gravity compensator holds the weight of the stage using passive magnets and enables actuation using a coil on the LS side. The magnets minimise power consumption for carrying the weight, but risk the adding of actuator stiffness. As the long-stroke stage is envisioned to be a conventional stage without high requirements, the transfer of disturbances should be minimised. To realise this, a low-stiffness actuator between the SS stage and LS stage was required, featuring typically less than 1,000 N/m per actuator.

A zero-stiffness gravity compensator has been designed consisting of a disc and a ring magnet as shown in Figure 7. The low-stiffness effect was realised by the hole in the center of the ring magnet. This hole can be seen as the superposition of a larger circular magnet combined with a smaller magnet polarised in opposite direction. The forces realising the low stiffness are graphically illustrated in Figure 8. The larger magnet with opposing magnetisation generates a repulsive force, F_1, while the smaller magnet with attractive polarisation creates an attraction force, F_2. The force F_2 has a steeper slope as the magnets come closer. By careful dimensioning, the sum of the force, F_3, exhibits the desired zero-stiffness effect. A circular coil has been added to the design to enable actuation.

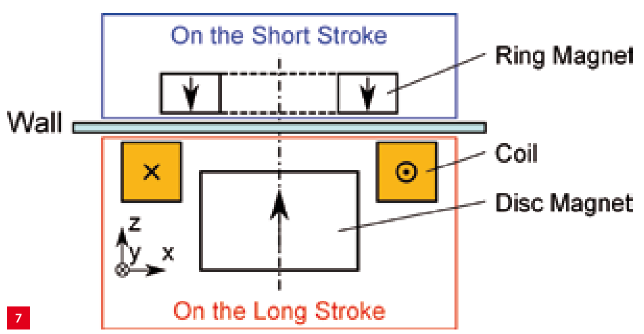

7

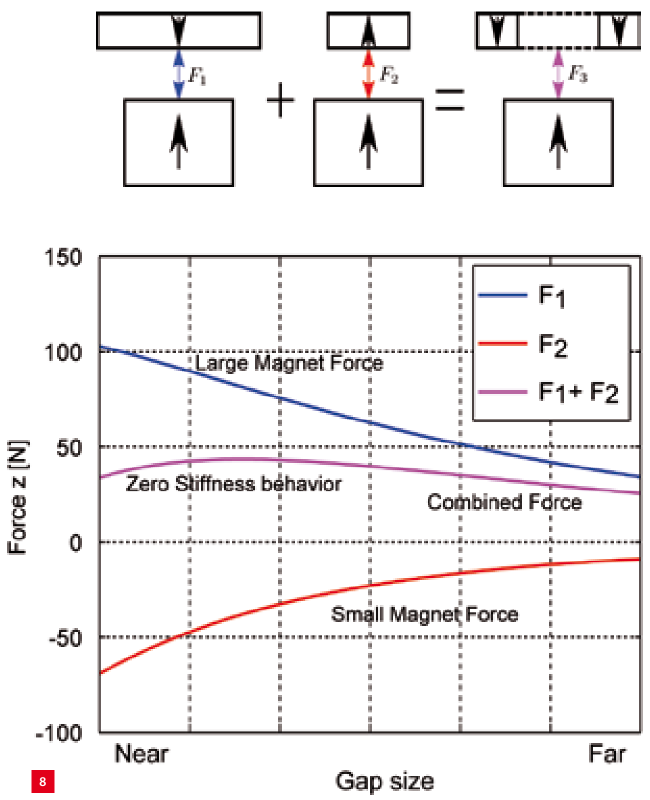

8

9 *Measured forces of active magnetic gravity compensator. (a) Force versus current. (b) Force versus position at I = 0 A. This shows close-to-zero stiffness at 5 mm gap.*
10 *Overview of designed demonstrator.*
11 *Exploded view of the through-wall demonstrator. SS only holds permanent magnets. LS is driven by a screw spindle.*

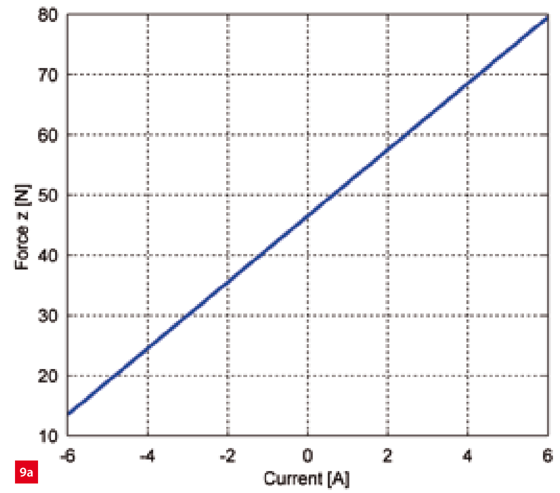

9a

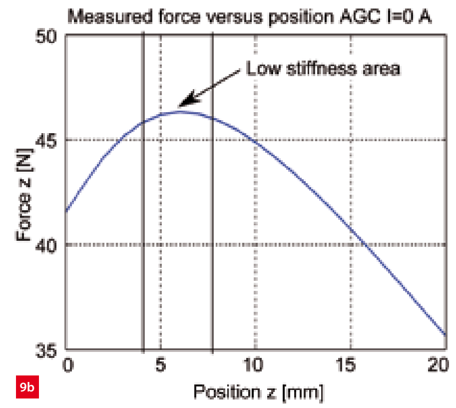

9b

To optimise the design of the actuator, the influence of various parameters has been analysed. These parameters consisted of the ring's inner and outer diameter, its thickness, as well as the disc's diameter and thickness. The optimisation was performed using an axisymmetric FEM (finite-element model) analysis. In this model only the out-of-plane force and stiffness can be calculated. The in-plane stiffness can then be calculated using Earnshaw's theorem [4]. From this theorem it can be deducted that the out-of-plane stiffness is equal to twice the in-plane stiffness with the sign inverted. This shows that a low vertical stiffness will directly lead to a low in-plane stiffness as well. The location of the zero stiffness can be adjusted by changing the diameters, while the amount of force is dictated by the thickness of the magnets. For the final design of the actuator only off-the-shelf magnets have been used.

Figure 9 shows the measured force versus position and current. The figure clearly displays the zero-stiffness behaviour of the actuator. Each of the actuators will carry 46 N of gravity load.

Mechanical design

To demonstrate the potential of the through-wall concept, a demonstrator has been realised. The demonstrator consists of the following elements: the SS, the LS, the wall, a metrology frame and a force frame as depicted in Figure 10. The goal of the demonstrator is not to reach nanometer precision but to show the concept and use it as an exhibition demonstrator. The design consists of a 500 mm x 500 mm SS wafer chuck, making it compatible with the newest generation of 450 mm wafers. No wires run to the chuck and it contains the magnets for in-plane and out-of-plane

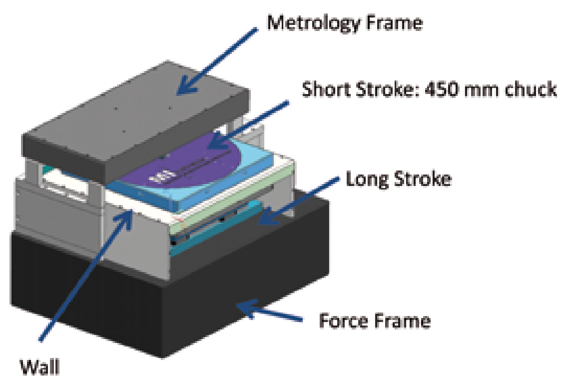

10

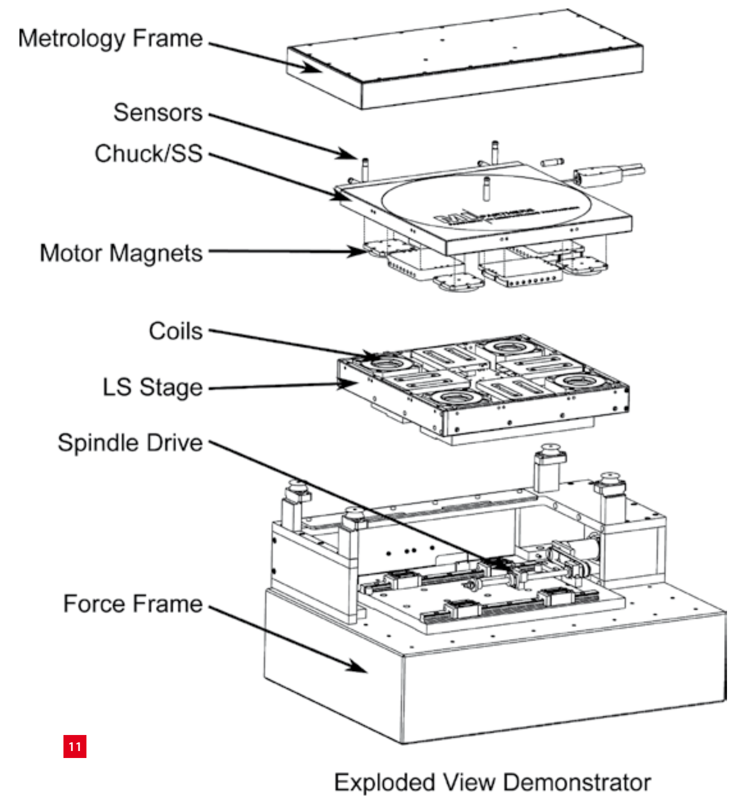

11

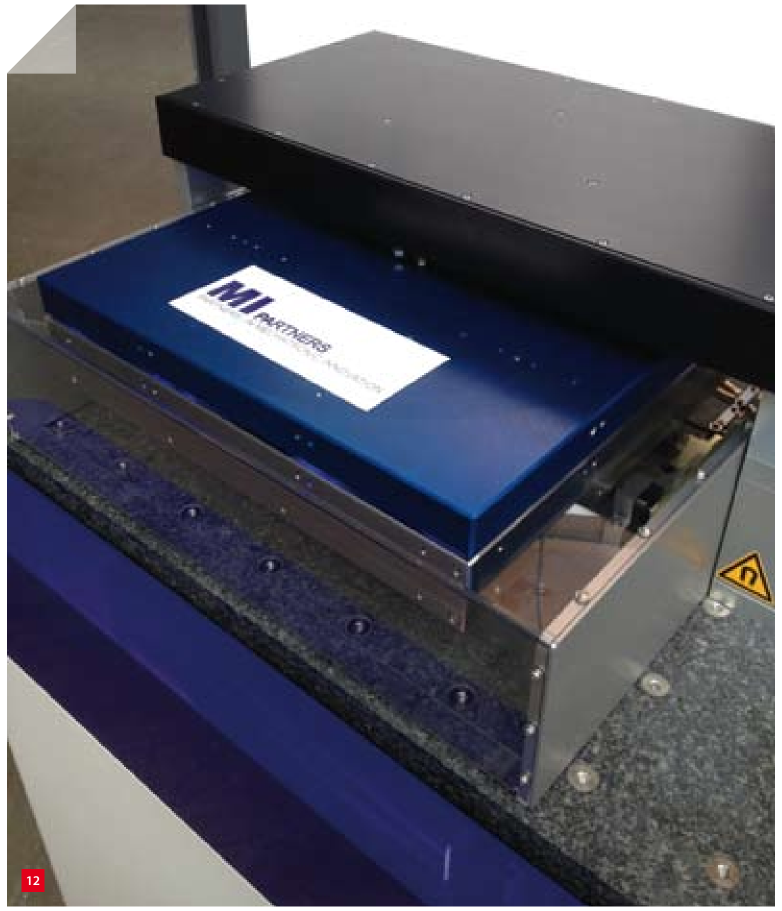

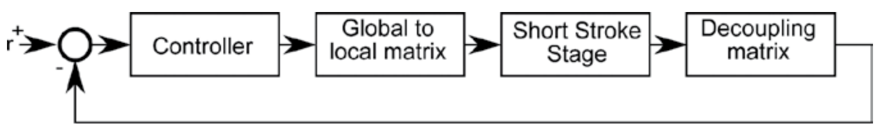

12 *The demonstrator at an exhibition.*

13 *Control architecture of SS stage. Decoupling occurs around its center of gravity.*

actuation. The demonstrator is not a vacuum system, but its components are vacuum compatible. An exploded view of the system is shown in Figure 11.

To measure the chuck, the metrology frame holds five eddy-current sensors and one laser interferometer. An additional eddy current is present for start-up purposes. The metrology frame is suspended on four rubber mounts. For the demonstrator system a suspension frequency between 10-15 Hz was selected. This is a trade-off between the filtering effect and practical stability of the frame as it will be used as an exhibition demonstrator.

On the granite base the LS stage is positioned. Due to the low stiffness of the actuators, vibrations on the LS stage only lead to small disturbance forces on the SS chuck. This allows the stage to be actuated by a simple screw spindle. Its position is measured by a linear encoder. Currently, the design has only one long-stroke direction, but a stacked XY stage can easily be added to the system to facilitate additional motion. Figure 12 shows a picture of the demonstrator at an exhibition.

Control results

To control the stage, the local measurements are decoupled around the centre of gravity of the chuck by use of a transformation matrix. The SS stage is controlled with six individually tuned PID controllers and forces distributed to the actuators by use of an actuator transformation. The layout of the control scheme for the SS stage is shown in Figure 13. The LS stage is controlled with respect to the force frame and obtains the same set-point as the SS stage, allowing it to roughly follow the motion of the SS stage.

The bandwidth of the SS stage was tuned to 100 Hz in all directions. The plant transfers in X- and Z-direction of the SS stage are shown in Figure 14. In Z-direction, the torsional modes of the chuck are only mildly excited and are hardly present in the FRF (Frequency Response Function). The main limitation is formed by the umbrella mode at 550 Hz. In X-direction, around 10 Hz excitation of the metrology frame can be seen; internal dynamics of the LS stage are not visible. The bandwidth-limiting modes are located at 900 Hz.

The position stability of the stage is in the order of a micrometer; this is mainly limited by the resolution of the eddy-current sensors as they have been selected to operate over a large range. By using a different sensing method, the performance of the stage can be improved to nanometer level. In Figure 15, the acceleration profile for a 10 cm set-point for a combined motion (LS+SS) is shown. The servo error of this set-point is also shown in Figure 15. The LS stage makes considerable errors that do not influence the tracking error of the SS stage. A frequency component of around 10 Hz can be seen in the servo error of the SS stage, which is caused by the excitation of the metrology frame by the set-point reaction forces.

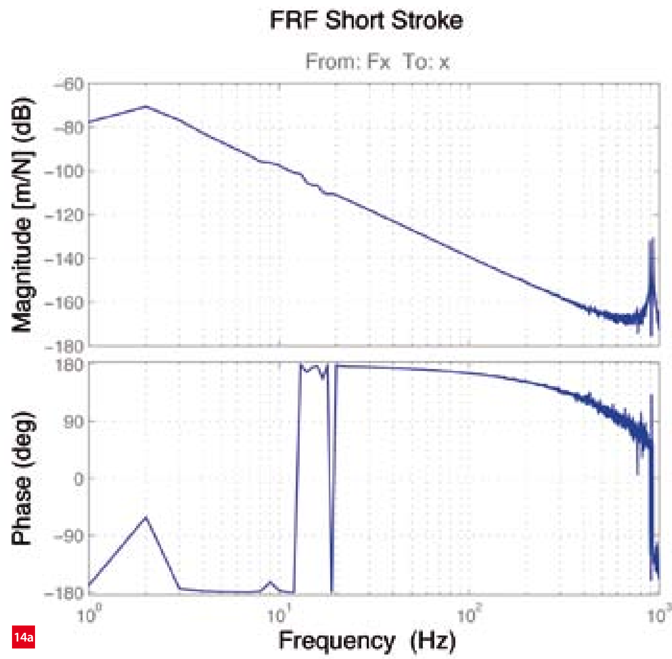

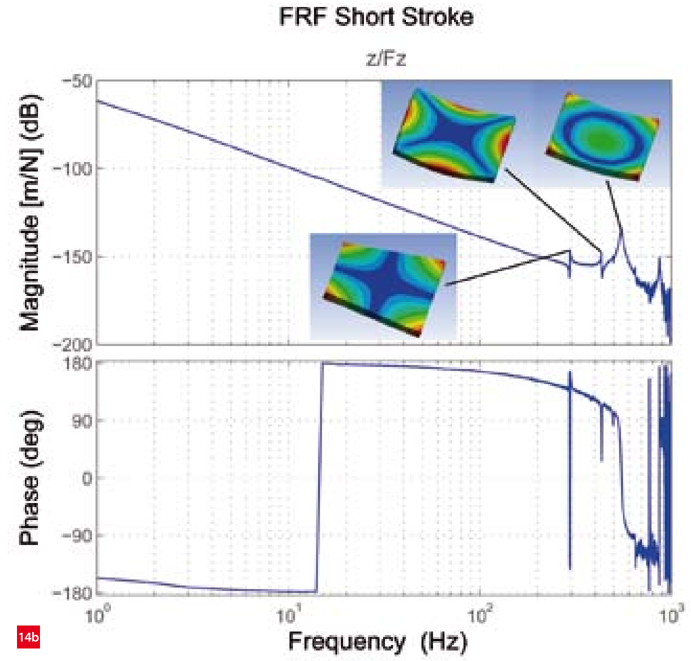

Conclusions & Outlook

The through-wall stage enables wireless actuation in a vacuum environment with promising performance. The application of over-actuation enables high dynamic performance for a relatively lightweight/flexible chuck. Integration of the system with a 6-DoF laser interferometer system will allow it to perform at nanometer level. Some form of wireless energy transfer will be required to allow for wafer clamping. At this moment, several customers have shown interest in the concept. MI-Partners is looking for cooperation with potential stage suppliers or OEMs for further development of the platform. ■

REFERENCES

[1] J.W. Jansen. "Magnetically levitated planar actuator with moving magnets: Electromechanical analysis and design", Ph.D. thesis, Eindhoven University of Technology, 2007.

[2] D. Laro, R. Boshuizen, and J. van Eijk. "Design and control of over-actuated lightweight 450 mm wafer chuck", *Proc. ASPE Control Topical Meeting*, 2010.

[3] H. Allag, J.P. Yonnet, and M.E.H. Latreche. "3D Analytical Calculation of Forces between Linear Halbach-Type Permanent Magnet Arrays", *Electromotion*, 2009.

[4] S. Earnshaw. "On the Nature of the Molecular Forces which Regulate the Constitution of the Luminiferous Ether". *Trans. Camb. Phil. Soc.* 7: 97-112, 1842.

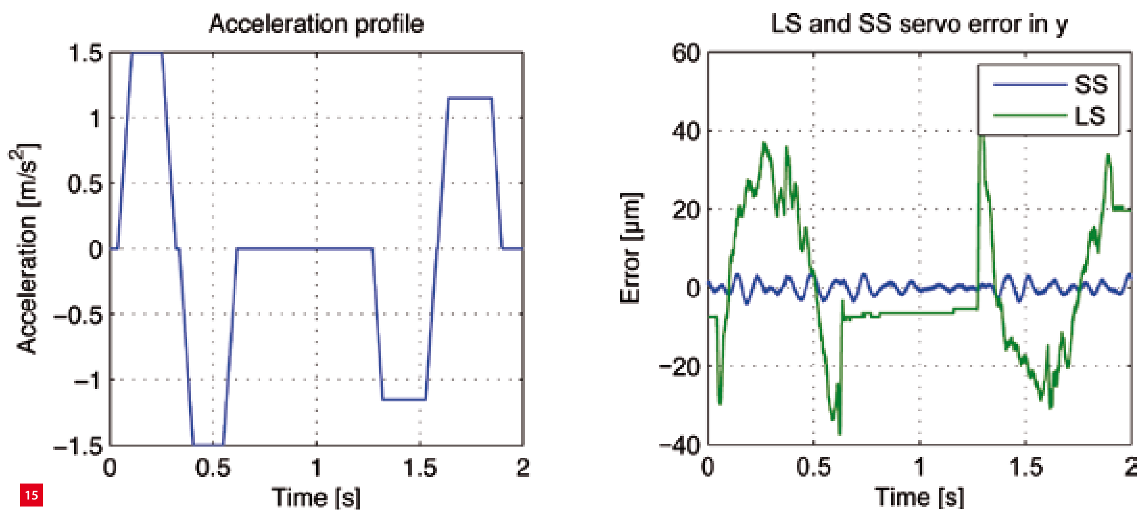

14 *Plant FRF of SS stage. (a) In X-direction. (b) In Z-direction.*

15 *Set-point tracking performance in horizontal direction for 10 cm set-point for given acceleration profile. Tracking errors on SS stage are unrelated to errors of LS stage.*